



Functional Cobalt Oxides

FUNDAMENTALS, PROPERTIES, AND APPLICATIONS

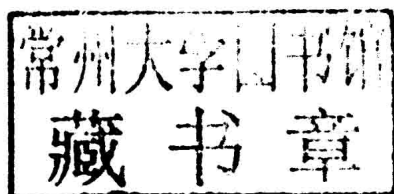
Tsuyoshi Takami



Functional Cobalt Oxides

FUNDAMENTALS, PROPERTIES, AND APPLICATIONS

Tsuyoshi Takami



PAN STANFORD  PUBLISHING

Published by

Pan Stanford Publishing Pte. Ltd.
Penthouse Level, Suntec Tower 3
8 Temasek Boulevard
Singapore 038988

Email: editorial@panstanford.com

Web: www.panstanford.com

British Library Cataloguing-in-Publication Data

A catalogue record for this book is available from the British Library.

Functional Cobalt Oxides: Fundamentals, Properties, and Applications

Copyright © 2014 Pan Stanford Publishing Pte. Ltd.

All rights reserved. This book, or parts thereof, may not be reproduced in any form or by any means, electronic or mechanical, including photocopying, recording or any information storage and retrieval system now known or to be invented, without written permission from the publisher.

For photocopying of material in this volume, please pay a copying fee through the Copyright Clearance Center, Inc., 222 Rosewood Drive, Danvers, MA 01923, USA. In this case permission to photocopy is not required from the publisher.

ISBN 978-981-4463-32-4 (Hardcover)

ISBN 978-981-4463-33-1 (eBook)

Printed in the USA



Functional Cobalt Oxides

Preface

When one looks around, one's apparels are found to made of many materials, which are said to reach 50,000 varieties. Surprisingly, these materials are composed of at most about 50 kinds of elements. Among them, the transition metals have a high melting point, high density, and multivalence. This book deals with oxide materials, including the transition metal Co, but the elementary Co itself with the 29th Clarke number exhibits ferromagnetism, as well as Ni and Fe, and has been used as a dye and a pigment to produce the well-known cobalt blue. There is a view according to which Co was designated by H. Brandt in 1735, and its name stems from German word "*Kobold*." In this connection, I may add that the name appears in a worldwide animation, *Mightly Atom*, created by O. Tezuka, as the name of the brother of the main character, Atom. Moreover, Co has been also widely used as alloys with Fe, Ni, and Cr: Ni-Fe-Co alloy is employed as a binder between glass and metal and Cr-Co-W alloy is dental or surgery material.

The book is motivated by the desire to describe why cobalt oxides have drawn much interest as functional materials, together with their peculiar physical properties partially originating from a rich variety of valences and spin states of Co ions. The leading role of the physical phenomena dealt with in this book is owed to the electron. The electron, discovered by J. J. Thomson in 1897, is a particle that cannot be far resolved under normal conditions and has a wave nature as well. Wave-particle duality was evidenced by experiments using the double split performed by C. Jönsson, P. G. Merli, and A. Tonomura in 1961, 1974, and 1989, respectively.

In the Co oxide system, the strong correlation between electrons generally plays a substantial role, where the conventional one-electron approximation fails. In particular, the characteristics of

Co ions in oxides should be focused on in comparison with other transition metals. This book starts with the basis of one-electron band theory and advances toward the stage of strong electron correlation systems and furthermore progresses to cover up-to-date topics such as huge thermoelectric power, superconductivity, and intrinsic inhomogeneity, etc. This book would be of interest to graduate students and researchers in the fields of physics, chemistry, and materials science. Aside from helping readers in the pencil-and-paper solution of problems, the discussion, which this book aims at developing, may be useful for understanding the essence of functional materials.

Tsuyoshi Takami

Acknowledgments

I acknowledge support from the Foundation of a Grant-in-Aid for Young Scientists (B) (Grant No. 21740251 and No. 24740233), Ando Laboratory, Thermal & Electric Energy Technology Foundation, Japan Society for the Promotion of Science (JSPS) Research Fellowships for Young Scientists, the Sasakawa Scientific Research Grant from the Japan Science Society, and the Research Foundation for the Electrotechnology of Chubu. It's thanks to Emeritus Prof. Uichiro Mizutani, Prof. Hiroshi Ikuta, and Dr. Jun Sugiyama that our achievements were successfully obtained and became worthy to be published as this book. Furthermore, I appreciate Profs. Tsunehiro Takeuchi, Jinguang Cheng, and Masayuki Itoh and Dr. Hiroshi Nozaki for their collaboration. Profs. John B. Goodenough and Jianshi Zhou are also thanked for useful discussions. I am indebted to Mr. Sarabjeet Garcha, senior editorial manager of Pan Stanford Publishing Pte. Ltd., for his advice on form and assistance for preparation. I appreciate Mr. Stanford Chong, director and publisher of Pan Stanford Publishing Pte. Ltd., for inviting me to develop my research topic into this book.

Tsuyoshi Takami

Contents

<i>Preface</i>	vii
<i>Acknowledgments</i>	ix
1 Introduction	1
1.1 Prologue	1
1.2 Charge, Spin, and Orbitals	1
1.3 Physical Properties under External Perturbations	12
2 Spin-State Crossover	27
2.1 Prologue	27
2.2 Valence and Spin State of Co Ions	28
2.3 Spin-State Crossover	31
2.4 Metal-Insulator Transition	39
2.5 Thermal Rectifier	40
3 Li Ion Battery	45
3.1 Prologue	45
3.2 History of Batteries	46
3.3 LiCoO_2 Batteries	48
4 Huge Thermoelectric Power	57
4.1 Prologue	57
4.2 Thermoelectric Materials	58
4.3 Na_xCoO_2	61
4.4 Other Co Oxides	63
4.5 Origin of a Huge Thermoelectric Power	64
4.6 Application	71
5 Room-Temperature Ferromagnetism	75
5.1 Prologue	75

5.2	Ferromagnetism in Transition Metal Oxides	78
5.3	Room-Temperature Ferromagnetism of $(\text{Sr,Y})\text{CoO}_{3-\delta}$	79
6	Partially Disordered Antiferromagnetic Transition	85
6.1	Prologue	85
6.2	Magnetism of $\text{Ca}_3\text{Co}_2\text{O}_6$	87
6.3	Magnetism of Quasi-1D $A_{n+2}\text{Co}_{n+1}\text{O}_{3n+3}$	92
7	Superconductivity	109
7.1	Prologue	109
7.2	Bose–Einstein Condensation	110
7.3	High- T_c Cuprate Superconductors	112
7.4	Superconductivity of $\text{Na}_x\text{CoO}_2 \cdot y\text{H}_2\text{O}$	115
8	Transport Properties Combined with Charge, Spin, and Orbital: Magnetoresistance and Spin Blockade	121
8.1	Prologue	121
8.2	The Magnetoresistance Effect	122
8.3	Magnetoresistance of $\text{RBaCo}_2\text{O}_{5.5}$	127
8.4	Extremely Large Magnetoresistance of PdCoO_2	130
8.5	Spin Blockade	131
9	Intrinsic Inhomogeneity	137
9.1	Prologue	137
9.2	Spin Cluster	140
9.3	Polaron Cluster	142
9.4	Phase Separation	144
9.4.1	Metallic and Semiconducting Phases	144
9.4.2	Spin-Density Wave and Ferromagnetic Phases	148
10	Move/Diffuse and Charge/Discharge Effect	155
10.1	Prologue	155
10.2	Cathode Material of Solid Oxide Fuel Cell: $\text{Sr}_{0.7}\text{Y}_{0.3}\text{CoO}_{2.63}$	157
10.3	Oxygen Storage Material: $\text{YBaCo}_4\text{O}_{7+\delta}$	162
	<i>Index</i>	165

Chapter 1

Introduction

1.1 Prologue

Cobalt oxides are known to exhibit peculiar physical/chemical properties, as well as being suitable candidates for wide applications such as electrode materials, thermoelectric materials, solid oxide fuel cells, and so forth. Such properties are closely related to versatility of the cobalt cations to adopt different valences and spin states in the narrow energy range, which associate with the charge and spin configuration on $3d$ orbitals, respectively. In this chapter, the charge, spin, and orbital for the $3d$ electron system are introduced, and then their role in the transport properties under external perturbations is formulated.

1.2 Charge, Spin, and Orbitals

Since electrons in materials are attracted by an atomic nucleus, their characteristics depend on the kind of elements and orbitals. The elements generally show the tendency given in Table 1.1. The density of conduction electrons $\rho(r)$ at a distance r from a certain atom deviates from the initial $\rho_0(r)$, and the potential $\varphi(r)$ and $\rho(r)$

Table 1.1 Characteristics of representative elements

	Alkaline metal	Transition metal	Actinoid metal	Rare-earth metal
Orbital	s	$3d$	$5f$	$4f$
Element	K, Na, ...	Fe, Co, ...	Pa, U, ...	Ce, Pr, ...
Extension of the wave function	large	middle	middle	small
Characteristic	itinerant	itinerant/localized	itinerant	localized
Electron correlation	weak	strong	midrange	strong

are connected with the Poisson equation:

$$\nabla^2 \varphi = -4\pi e^2 \rho(r) - \rho_0(r), \tag{1.1}$$

The proportional relationship of $(2\pi/L)^3 : 2 = 4\pi k_F^3/3 : N_A$ leads to

$$k_F = 3\pi^2 (N_A/V)^{1/3} = (3\pi^2 \rho(r))^{1/3}, \tag{1.2}$$

where L , k_F , N_A , and V are the edge length, the radius of the Fermi sphere, the Avogadro number, and the volume, respectively. Thus,

$$E_F + \varphi(r) = \left(\frac{\hbar}{2m} \right) (3\pi^2 \rho(r))^{2/3} \tag{1.3}$$

holds, which is converted to

$$\rho(r) = \frac{1}{3\pi^2} \left(\frac{2m}{\hbar} \right)^{3/2} E_F^{3/2} \left(1 + \frac{\varphi}{E_F} \right)^{3/2}, \tag{1.4}$$

where E_F and \hbar are the Fermi energy and the Planck's constant, respectively. By applying the Taylor expansion, this equation can be written as

$$\rho(r) = \rho_0 \left(1 + \frac{3}{2} \frac{\varphi}{E_F} \right), \tag{1.5}$$

where $\rho_0 = (1/3\pi^2)(2m/\hbar^2)^{3/2} E_F^{3/2}$.

Insertion into Eq. 1.1 gives

$$\nabla^2 \varphi = -\lambda^2 \varphi, \tag{1.6}$$

where $\lambda = (6\pi e^2 \rho_0/E_F)^{1/2}$. This equation is a function of the radius parameter r in the spherical coordinate and is rewritten as

$$\frac{1}{r^2} \frac{d}{dr} \left(r^2 \frac{d\varphi(r)}{dr} \right) = \lambda^2 \varphi(r), \tag{1.7}$$

and thus it can be confirmed that its solution becomes

$$\varphi(r) = -\frac{e^2 \Delta Z \exp(\lambda r)}{r^2}, \quad (1.8)$$

where ΔZ is the difference of the amount of charge. The parameter λ is called the Thomas–Fermi screening parameter. For instance, for the Co element alone, the insertion of $E_F = 7.4$ eV and $\rho_0 = 9.1 \times 10^{22} / \text{cm}^3$ gives $1/\lambda = 0.55$ Å. On the other hand, the intratomic distance equals the lattice constant a of 2.51 Å. Consequently, one can realize how effective the screening effect is because of $1/\lambda \ll a$.

For strongly correlated electron systems, since the scattering effect is less effective, three internal degrees of freedom of electrons, that is, charge, spin, and orbital, can be attributable to physical properties, which cannot be explained by a conventional band picture. When such degeneracies functionate on the crystal lattice, various electronic phases are formed. Charge is one of the properties of an elementary particle, and its quantity takes a positive sign or negative sign corresponding to the electron or the hole, respectively. The spin angular momentum is the angular momentum of elementary particles such as electrons and quarks, and complex particles possess one of the quantum degeneracies. On the other hand, the wave function is called orbital as a quantum dynamical concept corresponding to an orbit for classical electrons. Both the spin and the orbital angular momentum are ascribed to the total angular momentum of particles.

The Schrödinger equation is written as

$$\mathcal{H}\psi(\mathbf{r}) = E\psi(\mathbf{r}), \quad (1.9)$$

using the Hamiltonian defined as

$$\mathcal{H} = -\frac{\hbar^2}{2m_e} \nabla^2 + V(r). \quad (1.10)$$

Now, as long as the wave function is written as $\psi(\mathbf{r}) = f(r)Y(\theta, \varphi)$, the radial and angle wave equations are, respectively, given by

$$\frac{1}{\sin\theta} \frac{\partial}{\partial\theta} \left(\sin\theta \frac{\partial}{\partial\theta} \right) + \frac{1}{\sin^2\theta} \frac{\partial^2}{\partial\varphi^2} Y(\theta, \varphi) + \chi Y(\theta, \varphi) = 0 \quad (1.11)$$

and

$$\frac{1}{r^2} \frac{d}{dr} \left(r^2 \frac{d}{dr} \right) + \frac{2m}{\hbar^2} \left(E - V(r) - \frac{\chi}{r^2} \right) f(r) = 0, \quad (1.12)$$

where $\chi (= l(l+1))$ is a constant with no dimension. Furthermore, by using the relationship of $Y(\theta, \varphi) = \Theta(\theta)\Phi(\varphi)$, Eq. 1.11 is converted to

$$\frac{d^2\Phi}{d\varphi^2} + \nu\Phi = 0 \quad (1.13)$$

and

$$\frac{1}{\sin\theta} \frac{d}{d\theta} \left(\sin\theta \frac{d\Phi}{d\theta} \right) + \left(\chi - \frac{\nu}{\sin^2\theta} \right) \Phi = 0. \quad (1.14)$$

The solution of Eq. 1.13 is

$$\Phi = \frac{1}{\sqrt{2\pi}} \exp(im\varphi), \quad (1.15)$$

where $\nu = m^2$.

On the other hand, Eq. 1.14 is rewritten as

$$\frac{d}{d\omega} (1 - \omega^2) \frac{dP}{d\omega} + \left(\chi - \frac{m^2}{1 - \omega^2} \right) P = 0, \quad (1.16)$$

where $\omega = \cos\theta$. P is called the associated Legendre function and is specified as

$$P_l^m(\omega) = (1 - \omega^2)^{1/2|m|} \frac{d^{|m|}}{d\omega^{|m|}} P_l(\omega). \quad (1.17)$$

Thus,

$$Y_{l,m}(\theta, \varphi) = C_{l,m} P_l^m(\cos\theta) \Phi(\varphi) \quad (1.18)$$

$$= C_{l,m} P_l^m(\cos\theta) \frac{1}{\sqrt{2\pi}} \exp(im\varphi), \quad (1.19)$$

where

$$C_{l,m} = (-1)^{(m+|m|)/2} \frac{1}{\sqrt{2\pi}} \left[\frac{2l+1}{2} \frac{(l-|m|)!}{(l+|m|)!} \right]^{1/2}. \quad (1.20)$$

The wave function is finally expressed as

$$\varphi_{l,m} = f(r) Y_{l,m}(\theta, \varphi). \quad (1.21)$$

Therefore, the wave function of $3d$ orbitals for $(l, m) = (2, 0)$ is calculated as

$$\varphi_{2,0}(\mathbf{r}) = (-1)^0 \frac{1}{\sqrt{2\pi}} \sqrt{\frac{5}{2}} f \frac{1}{2^2 2!} (1 - \cos\theta)^0 \frac{d^2}{d^2 \cos\theta} (\cos^2\theta - 1)^2 \quad (1.22)$$

$$= \sqrt{\frac{5}{16\pi}} f (3\cos^2\theta - 1) \quad (1.23)$$

$$= \sqrt{\frac{5}{16\pi}} f \frac{1}{r^2} (3z^2 - r^2). \quad (1.24)$$

Please note here the relationship of $x = r\sin\theta\cos\varphi$, $y = r\sin\theta\sin\varphi$, and $z = r\cos\theta$. A similar procedure brings about

$$\varphi_{2,1\pm}(\mathbf{r}) = \sqrt{\frac{15}{4\pi}} f \frac{1}{r^2} z x, \sqrt{\frac{15}{4\pi}} f \frac{1}{r^2} y z \quad (1.25)$$

and

$$\varphi_{2,2\pm}(\mathbf{r}) = \sqrt{\frac{15}{16\pi}} f \frac{1}{r^2} (x^2 - y^2), \sqrt{\frac{15}{16\pi}} f \frac{1}{r^2} x y. \quad (1.26)$$

Among them, the relative probability fixed by the last wave function, where electrons distribute, is proportional to $(x^2 y^2 =) \sin^4\theta \cos^2\varphi \sin^2\varphi$. As shown in Fig. 1.1a, $\sin^4\theta$ mainly has finite values around $\pi/2$ and $3/2\pi$, which means most electrons disperse on the x - y plane. What is more, the $\cos^2\varphi \sin^2\varphi$ curve in Fig. 1.1b suggests that electrons spread over toward a diagonal-line direction (see also $3d_{xy}$ in Fig. 1.2). Five orbitals $\varphi_{2,0}(r)$, $\varphi_{2,1\pm}(r)$, and $\varphi_{2,2\pm}(r)$ are degenerate, but they are known to split into lower levels (t_{2g}) and higher levels (e_g) in the case of the ideal MO_6 octahedron due to the crystal field splitting. This orbital splitting can be interpreted intuitively as follows: $3z^2-r^2$ and x^2-y^2 orbitals in the e_g level turn to the position of O^{2-} ions (see Fig. 1.2). Coulomb interaction becomes strong due to negative charges at a close range, resulting in the e_g orbitals relatively going up compared to the t_{2g} orbitals.

More quantitatively, in the case of trigonal symmetry, the whole electric field is

$$V(\mathbf{r}) = V_2^0 + V_4^0 + V_4^3 \quad (1.27)$$

$$= A_2^0(3z^2 - r^2) + A_4^0(35z^4 - 30z^2r^2 + 3r^4) + A_4^3(x^3 - 3xy^2)z \quad (1.28)$$

and each component is written as

$$\sum (3z^2 - r^2) = \alpha \langle r^2 \rangle [3L_z^2 - L(L+1)], \quad (1.29)$$

$$\begin{aligned} \sum (35z^4 - 30z^2r^2 + 3r^4) &= \beta \langle r^4 \rangle [35L_z^4 - 30L(L+1)L_z^2 \\ &\quad + 25L_z^2 - 6L(L+1) + 3L^2(L+1)^2], \end{aligned} \quad (1.30)$$

and

$$\sum (x^3 - 3xy^2)z = \frac{\beta}{4} \langle r^4 \rangle [L_z(L_+^3 + L_-^3) + (L_+^3 + L_-^3)L_z]. \quad (1.31)$$

Hereafter, let's calculate the detailed energy level. First we estimate V_4^3 , including the matrix element.

$$L_+^2 = \begin{pmatrix} 0 & 2 & 0 & 0 & 0 \\ 0 & 0 & \sqrt{6} & 0 & 0 \\ 0 & 0 & 0 & \sqrt{6} & 0 \\ 0 & 0 & 0 & 0 & 2 \\ 0 & 0 & 0 & 0 & 0 \end{pmatrix} \begin{pmatrix} 0 & 2 & 0 & 0 & 0 \\ 0 & 0 & \sqrt{6} & 0 & 0 \\ 0 & 0 & 0 & \sqrt{6} & 0 \\ 0 & 0 & 0 & 0 & 2 \\ 0 & 0 & 0 & 0 & 0 \end{pmatrix} = \begin{pmatrix} 0 & 0 & 2\sqrt{6} & 0 & 0 \\ 0 & 0 & 0 & 6 & 0 \\ 0 & 0 & 0 & 0 & 2\sqrt{6} \\ 0 & 0 & 0 & 0 & 0 \\ 0 & 0 & 0 & 0 & 0 \end{pmatrix} \quad (1.32)$$

$$L_+^3 = \begin{pmatrix} 0 & 0 & 0 & 12 & 0 \\ 0 & 0 & 0 & 0 & 12 \\ 0 & 0 & 0 & 0 & 0 \\ 0 & 0 & 0 & 0 & 0 \\ 0 & 0 & 0 & 0 & 0 \end{pmatrix} \quad (1.33)$$

A symmetric procedure on the matrix elements brings about

$$L_-^3 = \begin{pmatrix} 0 & 0 & 0 & 0 & 0 \\ 0 & 0 & 0 & 0 & 0 \\ 0 & 0 & 0 & 0 & 0 \\ 12 & 0 & 0 & 0 & 0 \\ 0 & 12 & 0 & 0 & 0 \end{pmatrix}. \quad (1.34)$$

The first and second terms in Eq. 1.31, respectively, become

$$\begin{aligned}
 L_z(L_+^3 + L_-^3) &= \begin{pmatrix} 2 & 0 & 0 & 0 & 0 \\ 0 & 1 & 0 & 0 & 0 \\ 0 & 0 & 0 & 0 & 0 \\ 0 & 0 & 0 & -1 & 0 \\ 0 & 0 & 0 & 0 & -2 \end{pmatrix} \begin{pmatrix} 0 & 0 & 0 & 12 & 0 \\ 0 & 0 & 0 & 0 & 12 \\ 0 & 0 & 0 & 0 & 0 \\ 12 & 0 & 0 & 0 & 0 \\ 0 & 12 & 0 & 0 & 0 \end{pmatrix} \\
 &= \begin{pmatrix} 0 & 0 & 0 & 24 & 0 \\ 0 & 0 & 0 & 0 & 12 \\ 0 & 0 & 0 & 0 & 0 \\ -12 & 0 & 0 & 0 & 0 \\ 0 & -24 & 0 & 0 & 0 \end{pmatrix} \quad (1.35)
 \end{aligned}$$

and

$$(L_+^3 + L_-^3)L_z = \begin{pmatrix} 0 & 0 & 0 & -12 & 0 \\ 0 & 0 & 0 & 0 & -24 \\ 0 & 0 & 0 & 0 & 0 \\ 24 & 0 & 0 & 0 & 0 \\ 0 & 12 & 0 & 0 & 0 \end{pmatrix}. \quad (1.36)$$

Thus,

$$L_z(L_+^3 + L_-^3) + (L_+^3 + L_-^3)L_z = \begin{pmatrix} 0 & 0 & 0 & 12 & 0 \\ 0 & 0 & 0 & 0 & -12 \\ 0 & 0 & 0 & 0 & 0 \\ 12 & 0 & 0 & 0 & 0 \\ 0 & -12 & 0 & 0 & 0 \end{pmatrix}. \quad (1.37)$$

For easy calculation of the eigenvalue, the matrix elements are rearranged in order of $M = 0, 1, -2, -1$, and 2 instead of the present alignment of $M = 2, 1, 0, -1$, and -2 .

$$L_z(L_+^3 + L_-^3) + (L_+^3 + L_-^3)L_z = \begin{pmatrix} 0 & 0 & 0 & 0 & 0 \\ 0 & 0 & -12 & 0 & 0 \\ 0 & -12 & 0 & 0 & 0 \\ 0 & 0 & 0 & 0 & 12 \\ 0 & 0 & 0 & 12 & 0 \end{pmatrix}. \quad (1.38)$$

Here we replace $-3A_2^0\alpha \langle r^2 \rangle = A$, $12A_4^0\beta \langle r^4 \rangle = B$, and $-3A_4^3\beta \langle r^4 \rangle = C$. The two residual electric fields are expressed as follows:

$$V_2^0 = \alpha \langle r^2 \rangle A_2^0(3M^2 - 6) \quad (1.39)$$

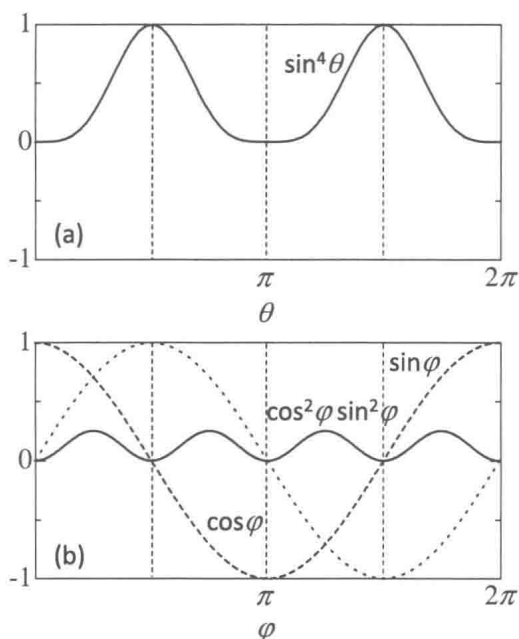


Figure 1.1 Functions of (a) $\sin^4 \theta$ and (b) $\cos^2 \varphi \sin^2 \varphi$ together with $\sin \varphi$ (dotted curve) and $\cos \varphi$ (dashed curve).

and

$$V_4^0 = \beta \langle r^4 \rangle A_4^0 (35M^4 - 155M^2 + 72), \quad (1.40)$$

and thereby

$$V_2^0 = \begin{cases} 2A & (M=0) \\ A & (M=1) \\ -2A & (M=-2) \\ A & (M=-1) \\ -2A & (M=2) \end{cases} \quad (1.41)$$

and

$$V_4^0 = \begin{cases} 6B & (M=0) \\ -4B & (M=1) \\ B & (M=-2) \\ -4B & (M=-1) \\ B & (M=2). \end{cases} \quad (1.42)$$